

Initial Data for Black Holes and Black Strings in 5d.

Evgeny Sorkin and Tsvi Piran

Racah Institute of Physics, The Hebrew University, Jerusalem, 91904, Israel.

(21.11.2002)

We explore time-symmetric hypersurfaces containing apparent horizons of black objects in a 5d spacetime with one coordinate compactified on a circle. We find a phase transition within the family of such hypersurfaces: the horizon has different topology for different parameters. The topology varies from S^3 to $S^2 \times S^1$. This phase transition is discontinuous – the topology of the horizon changes abruptly. We explore the behavior around the critical point and present a possible phase diagram.

Several black objects solutions exist in spacetimes with dimensionality greater than four containing compact dimensions. Among these solutions are black strings and black holes – two black objects with distinct horizon topology. However no general analytic solution is known for a black object in a compactified space-time in more than 4d spacetime.

Gregory and Laflamme (GL) [1,2] discovered that a uniform black string, a product of a Schwarzschild solution with a line, develops a dynamical instability if a compactification radius is 'too large'. They hypothesized that the endpoint of this instability would be a black-hole. Horowitz and Maeda [3,4] argued that the GL instability cannot cause a uniform black-string to decay to a black hole, at least in a finite affine time. This is because of the 'no tear' property of horizons. They conjectured that the endpoint of such a decay would be another phase of solutions – a non-uniform black string. Wiseman found numerically [5,6] non-uniform black-string solutions. However, Wiseman stresses that these solutions are most likely unstable.

We consider here the five dimensional spacetime with one compact dimension of length $2L$. We denote the coordinate along the compact dimension by z . A neutral black object has a characteristic dimensionfull parameter, its asymptotic 4d mass, M . It is convenient to describe the system by a single dimensionless parameter, $\zeta \equiv G_4 M / (2L)$, where the effective Newton constant is $G_4 = G_5 / 2L$. If $\zeta \ll 1$ the black object is expected to resemble a 5d Schwarzschild black-hole since local measurements cannot probe the compactness of the z direction. The horizon of this black-hole is therefore expected to have an S^3 topology. At the opposite end, $\zeta \gg 1$, one expects that the horizon would extend over the compact dimensions wrapping it completely. The horizon's topology of this object, $S^2 \times S^1$, suggests the name 'black string'. A uniform black-string is described by a 4d Schwarzschild solution times a circle. A non-uniform black-string is characterized by a non-trivial z -dependence along the circle. An attempt, based on a thermodynamical reasoning, to construct the phase diagram that would include consistently different phases of solutions was recently undertaken by Kol [7].

In this letter we make a step toward the self-consistent study of black objects in compact 5d background. We

solve numerically the initial-value problem for a moment of time-symmetry for spacetimes containing black objects. We determine the *apparent* horizon of the existing black objects in these solutions and we follow the transition from spherical to cylindrical topology in a family of solutions with a different dimensionless parameter ζ . Although the configurations we find are not 5d static solutions, these solutions, give us some insight on the behavior of the black objects in a compactified background. A similar approach was previously applied [8] to explore the time-symmetric black-hole problem in the brane world scenario.

We consider a time-symmetric slice through the black object's space-time. To generate the black object solution we consider a configuration with an artificial matter around the origin. This matter gives rise to a non-flat spatial metric along the slice. We solve numerically for this metric. Then we solve for the *apparent* horizon of the black object. The method allows us to determine the spatial geometry of the black object. Since we solve along a time-symmetric slice, this spatial geometry constitutes the initial data for subsequent dynamical time evolution of this black object's geometry. Limiting ourselves only to the determination of the initial data we find explicitly time-symmetric solutions with a distinct horizon topology and construct the phase diagram for a family of such solutions parametrized by ζ . We show that there is a phase transition within this family. We identify the critical ζ_c and show explicitly that if ζ_c is reached from below a corresponding black-hole solutions becomes deformed and the horizon has a cigar-like shape. If ζ_c is approached from above, the corresponding black-string solution becomes more and more non-uniform. However, this cannot be considered as evidence for existence of a non-uniform static black-string solutions. This initial data may relax to a uniform string during its dynamical evolution. We find that the transition between both topologies is not smooth: the spherical-like horizon jumps suddenly to become a cylindrical-like horizon. Put differently, neither the black-string pinches nor the black-hole has its south and north poles touching each other.

The method that we describe here enables us to study properties of black objects with different apparent horizon's topology in a single consistent numerical scheme. Our method does not require a prescription of the topol-

ogy of the horizon. The topology is not predetermined but rather it is a derived result of numerics. Usually, to obtain a *static* black object solution of the 5d Einstein equations one would had to specify the topology of the horizon. In other words there is no a single numerical scheme that can find black objects with distinct horizon topology.

Let us consider a time-symmetric, spacelike hypersurface Σ_t with a vanishing extrinsic curvature. The Hamiltonian constraint reads

$$R^{(4)} = 16\pi G_5 T_{\mu\nu} t^\mu t^\nu, \quad (1)$$

where t^μ is the unit normal to Σ_t and $T_{\mu\nu}$ is the 5d stress-energy tensor. From now on we work in units where $c = G_5 = 1$. The momentum constraint is trivially satisfied provided that the matter is static and the extrinsic curvature of this slice vanishes.

We choose the metric on Σ_t to be conformally flat

$$dl^2 = \psi^2(dr^2 + dz^2 + r^2 d\Omega_2^2). \quad (2)$$

This ansatz have been adopted for simplicity and more complicated choices will be considered later.

With this choice of the metric the constraint equation takes the form

$$\nabla^2 \psi + \rho \psi^3 = 0, \text{ where } \nabla^2 \equiv \frac{1}{r^2} \partial_r (r^2 \partial_r) + \partial_{zz}. \quad (3)$$

Here we have defined $\rho \equiv T_{\mu\nu} t^\mu t^\nu > 0$, the physical energy density. This ρ is some artificial (auxiliary), freely specified matter density, distributed around the origin. In practice, we pick a top-hat matter distribution that occupies some finite region around the origin. This artificial matter gives rise to a non-trivial ψ in a way that does not involve specifying an inner boundary of a black object. For sufficiently concentrated mass an apparent horizon appears. For lower values of ρ the solution describes a momentary static star.

To solve the elliptic Eqn (3) we have to specify boundary conditions. These conditions are: (i) At the equatorial plane, $z = 0$, we have a reflection b.c. $\partial_z \psi = 0$; (ii) At the symmetry axis, $r = 0$, we have also a reflection symmetry: $\partial_r \psi = 0$; (iii) Periodicity in z implies also reflection symmetry at $z = L$: $\partial_z \psi = 0$; (iv) At $r \rightarrow \infty$ we set $\psi \sim 1 + G_4 M / 4r$, which is consistent with the 4d asymptotic behavior*. This condition is implemented

*The asymptotic metric is expected to take the form of a 4d Schwarzschild times a line. This metric generally cannot be brought to the conformally flat form (2). However, asymptotically, as $r \rightarrow \infty$, a transformation is possible at the leading order. The asymptotic behavior of the conformal factor would become $\psi \sim 1 + MG_4/4r$. The length of the circle tends asymptotically to $2L$ so we can read the asymptotic 4d mass in the units of the effective Newton constant $G_4 = G_5/2L$.

by rewriting it as $\partial_r(r\psi) = 1$, eliminating the need to specify M . Instead, M is determined from the numerical solution.

There is a wide literature about equations like (4), see [9] and references therein. This equation is ill posed and it does not have a unique solution. In order to bring the equation to a well posed form we rescale the matter density $\rho \rightarrow \tilde{\rho} \psi^{-3-s}$, with some $s > 0$ and nonphysical density $\tilde{\rho}$, see e.g. [9]. The resulting equation

$$\nabla^2 \psi + \tilde{\rho} \psi^{-s} = 0 \quad (4)$$

is well posed and has a unique solution. The rescaling of the matter density is unimportant as we are interested only in the external vacuum part. The solution for ψ is found using relaxation.

We obtain a sequence of momentary time-symmetric solutions by fixing the density of the artificial matter and its location as $\tilde{\rho} = 10^6 \Theta(0.5 - r) \Theta(0.5 - z)$, and varying continuously the length of the compact asymptotic circle, $2L$. We used grids, covering the domain $0 < z < L$, and $0 < r < R_{max}$, with typical grid spacings of $\Delta r \sim 0.02$ and $\Delta z \sim 0.01$. The value of R_{max} , where the asymptotic b.c. (iv) was implemented, has been taken as $R_{max} = 5, 10$ and 20 . We checked that the results are insensitive to variation of R_{max} , provided that $R_{max} > 5$.

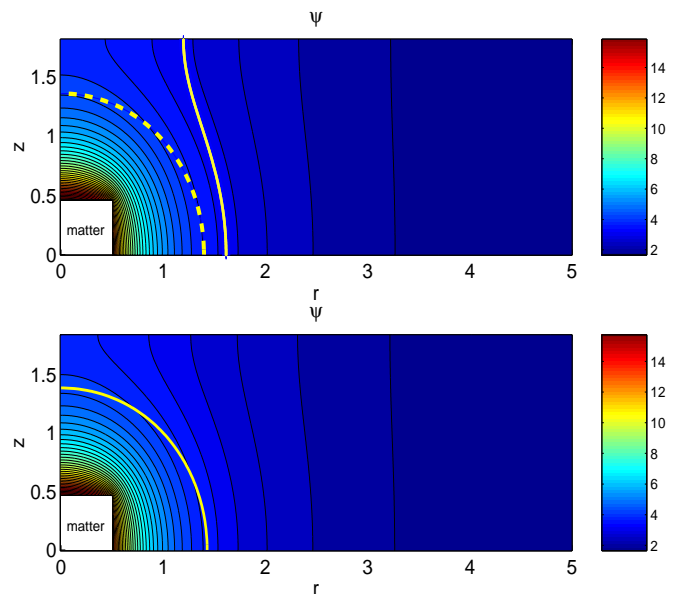


FIG. 1. Contours of ψ . Upper panel: $\zeta \simeq 7.25$ and there is a non-uniform black-string. Bottom panel: $\zeta \simeq 7.0$ and there is a black-hole. In both plots one observes how the deformation of the contour lines fades asymptotically. We plot also the apparent horizons in both cases. These are designated by thick curves. In the upper plot that corresponds to the black-string phase there are two horizons. The inner spherical apparent horizon, designated by the dotted thick curve, and the outer cylindrical horizon, designated by the solid curve.

To envisage the spatial metric around the black objects in Fig.1 we plot the contours of ψ in two cases that

correspond to a black-hole solution and a non-uniform black-string solution. The matter is located near the origin and is encircled by the horizon in either case. The geometry outside the apparent horizon has an axisymmetric structure and it becomes asymptotically flat. The ψ contour lines are spherical near the origin and become cylindrical as r increases. Because of the reflection symmetry both at the axis $r = 0$ and at $z = L$ there cannot be a ψ contour line that falls into the left upper corner. This suggests that the topology of contours does not change smoothly.

Once we obtain ψ we determine the existence of the apparent horizon. An apparent horizon is defined by a zero-expansion of the null rays generating the horizon [10]. For the time-symmetric hypersurface Σ_t this condition can be written as

$$\nabla_{\mu}^{(4)} n^{\mu} = 0, \quad (5)$$

where n^{μ} is the unit normal to the apparent horizon.

To simplify the treatment, we distinguish between two different topologies for the horizon.

(1) When the horizon has the topology $S^2 \times S^1$ we choose cylindrical coordinates (r, z) and we solve for a curve $r = h(z)$.

(2) When the horizon has the topology of S^3 it is convenient to transform to spherical coordinates R, χ defined by $r = R \sin(\chi), z = R \cos(\chi)$. The horizon in the R, χ plane is given by a curve $R = h(\chi)$.

The unit normal to the curve that defines the horizon is

$$n^{\mu} = (C, -Ch'). \quad (6)$$

The parameter $C(r, z)$ could be read from the normalization condition $n^{\mu} n_{\mu} = 1$. In both cases we solve numerically equation (5) to obtain the position of the apparent horizon.

A useful qualitative parameter employed as a measure of the non-uniformity of a black-string [11] is $\lambda \equiv 1/2(r_{max}/r_{min} - 1)$ where r_{min} and r_{max} are the minimal and the maximal 4d Schwarzschild radii of the apparent horizon. For a uniform string $\lambda = 0$. In the black-hole phase $\lambda = \infty$. Therefore, for a black-hole we define another parameter $\lambda' \equiv R_{max}/R_{min} - 1$, where R_{max} and R_{min} are the 5d Schwarzschild radii of the horizon. This parameter gives an idea of deformation of the black-hole's horizon.

We find that there are two topologically distinct apparent horizon solutions. At small ζ the topology of the horizon is S^3 and the horizon is close to be exactly spherical. When ζ increases we see that the horizon begins to deform, deviating from a spherical shape but still remaining topologically 3-sphere. At a certain value, $\zeta_m \simeq 7.17$, a phase transition takes place – the topology of the apparent horizon changes from S^3 to $S^2 \times S^1$. In fact there are two apparent horizons in the black-string phase. The outer horizon, has a cylindrical topology, while the inner one has a spherical topology. In Fig.2 we plot the

sequence of solutions parametrized by ζ . In this figure there are finite values of ζ when $\lambda = 0$ or $\lambda' = 0$. In fact for these ζ the deformation of the horizon becomes so small that cannot be resolved by our numerics and we put the corresponding lambdas to zero.

Another interesting result is the measure of geometrical deformation of the horizons. In the black-string and the black-hole phases this measure is supplied by λ and λ' respectively. The non-uniformity of the black-string is displayed in the upper panel of Fig. 2. Near the critical point the most non-uniform string has $\lambda \simeq 0.22$. The non-uniformity disappears as ζ increases. For $\zeta \geq 12.2$ the black-string becomes a uniform black-string. The deformation of the horizon in the black-hole phase could be seen in the bottom panel of the same Figure. The maximal radius, R_{max} , always occurs at the axis, $r = 0$. The black-hole becomes more and more oblate and stretched along the symmetry axis, as we approach the critical point. The most deformed black-hole has $\lambda' \simeq 0.15$ just before the transition.

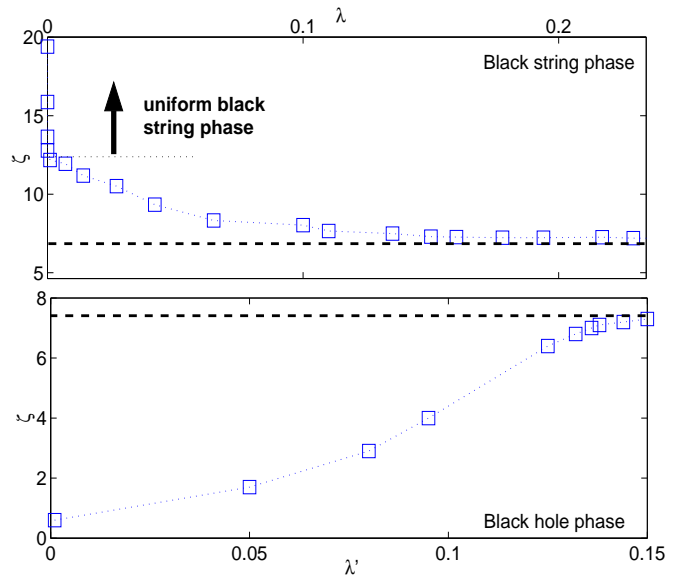


FIG. 2. The path in the configuration space of the numerical solutions. The black-hole phase is displayed in the bottom panel, the black-string phase is displayed in the upper panel. In both panels the horizontal dashed line that is located at $\zeta_c \simeq 7.17$ designates the *black-string* \rightarrow *black-hole* transition point. Above this line there is black-string phase, while below the line there is the black-hole phase. The black-string becomes uniform at $\zeta \simeq 12.2$ and the black-hole becomes spherical at $\zeta \simeq 0.61$.

The phase transition is discontinuous. At the critical value of ζ_c the spherical horizon jumps suddenly to become a cylindrical. To get insight on the behavior of the phase transition, in the black-hole phase we have computed the proper distance along the $r = 0$ axis from the black-hole horizon at the axis to $z = L$:

$$\ell = \int_{r(5)}^L \psi(r=0, z) dz . \quad (7)$$

This distance decreases as we increase ζ . One could expect that as horizon grows and as $\ell \rightarrow 0$ the north pole of the black-hole would tend towards its south pole and they will touch. However, we find that as $\zeta \rightarrow \zeta_c$ ℓ reaches a finite value. We plot the behavior of ℓ as a function of $\zeta - \zeta_c$ in Fig. 3. One observes that ℓ tends to a positive constant just before the transition.

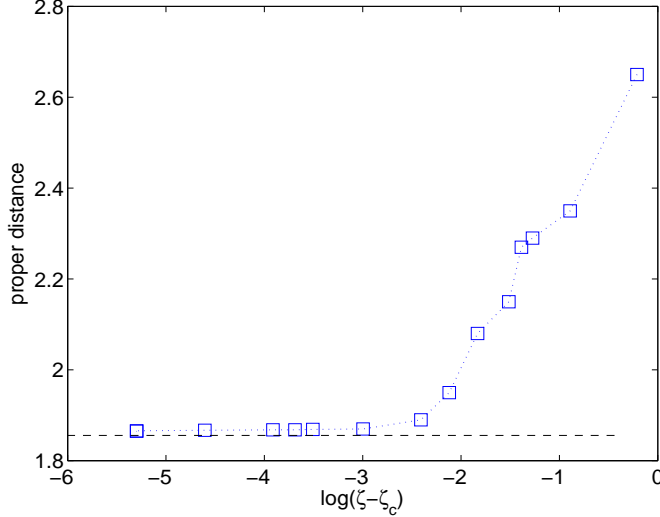


FIG. 3. The proper distance from the black-hole to the reflection plane $z = L$ does not decrease to zero but tends to a finite value as we approach the transition point.

The initial data that we have constructed here is similar in some extent to the Misner initial data [12] for a family of momentary static two equal mass black-holes in 4d GR. Misner choose a sequence of conformally flat metrics with the conformal factor parametrized by a certain parameter μ that is related to the mass of the black holes and their proper mutual separation. As μ varies the shape of the initial apparent horizons varies. If the black-holes are close enough, that occurs for small μ , a new apparent horizon suddenly appears, surrounding both black-holes on the initial hypersurface. In other words, there is a critical μ_0 that divides two distinct possibilities for the topology of the apparent horizon on the initial slice. Just by looking at this initial data sequence one has an indication that the event horizons for two black-holes will merge and form a distorted black-hole during an actual evolution. The value of μ when this merge occurs, generally would not coincide with the theoretical, μ_0 . In fact, the numerical evolution [13,14] of Misner initial data shows that the qualitative picture obtained for the sequence of the initial data is correct. The actual critical value of μ does not coincide with μ_0 , they are, however, not that different from each other.

Here we have an infinite array of black-holes that are approaching each other simultaneously. We have shown

that there is a family of initial data parametrized by ζ . When the separate black-holes in the array are getting closer they become distorted from the spherical shape. At a critical value ζ_c the separate horizons are engulfed suddenly by a single cylindrical-like horizon. The effective cylindrical horizon after the transition is non-uniform. The concrete numerical value of ζ_c isn't important as it is just a number characteristic to the specific initial data sequence. However we expect that the qualitative behavior would be similar in the static solutions as well. We believe that a dynamical evolution of our initial data would confirm this qualitative picture and will yield actual critical value, ζ_c .

Acknowledgment We thank Barak Kol for useful conversations. The research was supported by an ISF grant.

-
- [1] R.Gregory, R.Laflamme, Phys. Rev. Lett. **70**, (1993), 2837.
 - [2] R.Gregory, R.Laflamme, Nucl. Phys. **B428**, (1994), 399.
 - [3] G.Horowitz, K.Maeda, Phys.Rev.Lett.**87**, (2001), 130301.
 - [4] G.Horowitz, Playing with black strings (2002), [arXiv:hep-th/0205069].
 - [5] T.Wiseman, Static axisymmetric vacuum solutions and non-uniform black string (2002), [arXiv:hep-th/0209051].
 - [6] T.Wiseman, From Black strings to black holes (2002), [arXiv:hep-th/0211028].
 - [7] B.Kol, Topology change in general relativity and the black-hole black-string transition (2002), [arXiv: hep-th/0206220].
 - [8] T.Shiromizu and M.Shibata, Phys.Rev.D **62**, (2000) 127502
 - [9] J.W.York, in 'Sources of gravitational radiation', edited by Larry Smarr, Cambridge, 1979.
 - [10] S.W.Hawking and G.F.R Ellis, *The Large Scale Structure of Space-time* Cambridge University Press, 1973.
 - [11] S.Gubser, On non-uniform black branes, 2001, [arXiv: hep-th/0110193].
 - [12] C. W. Misner, Phys. Rev. **118**, (1960), 1110.
 - [13] P. Anninos *et.al.*, The head on collisions of two equal mass black holes: Numerical Methods, 1994, [arXiv gr-qc/9408042]; P. Anninos *et.al.*, Phys.Rev.Lett. **74**, (1995), 630.
 - [14] M. Alcubierre *et.al*, Phys. Rev. Lett. **87**, (2001), 271103.